ELSEVIER

Chemical Engineering Science 62 (2007) 5409–5417

Chemical Engineering Science

www.elsevier.com/locate/ces

Impact of vaporization in a residue hydroconversion process

Th. Gauthier*, J.P. Héraud, S. Kressmann, J. Verstraete

Institut Français du Pétrole, BP 3, 69390 Vernaison, France

Received 16 June 2006; received in revised form 20 December 2006; accepted 27 December 2006
Available online 25 January 2007

Abstract

Ebullated-bed hydroconversion is an important industrial process for upgrading of heavy feedstocks such as residues. The presence of a vapour phase in the reactor can significantly impact the hydroconversion performances, however. Bench unit data were used to collect vapour–liquid equilibrium data under reacting conditions and describe vaporization occurring in the reactors. Flash calculations were then conducted to check the ability of thermodynamic models to predict this equilibrium under industrial operating conditions. Finally, correctly accounting for vaporization is shown to be essential to accurately describe conversion kinetics.

Keywords: Ebullated bed; Residue conversion; Vaporization; Gas–liquid equilibrium; Reactor modelling

1. Introduction

Residue conversion processes are becoming increasingly important due to a declining market for residual fuel oil and an increasing demand for middle distillates and motor fuels. At the same time, the conventional crude oil market declines, whereas the non-conventional extra-heavy crude oil and tar sand bitumen market increases (Flint, 2004). Residue of heavy crude oils can be upgraded through various processes. Among these processes, the ebullated-bed catalytic hydroconversion process has the unique feature of deeply converting heavy feedstocks with high impurity contents while operating with a long cycle time (Colyar, 1997; Colyar and Wisdom, 1997; Duddy et al., 2004).

There is little information published in the literature reporting detailed studies of hydroconversion mechanisms occurring in the ebullated-bed reactor. Over the recent years, Nagaishi et al. (1997) have studied hydroconversion mechanisms in a batch reactor with multipass operation. McKnight et al. (2003) emphasized the importance of gas hold-up in industrial ebullated-bed reactors with respect to design aspects. Schweitzer and Kressmann (2004) proposed a detailed modelling of hydroconversion inside the ebullated bed, by considering an axial dispersion of liquids in a reactor combined with a four lump approach for the cracking mechanisms with first order reactions. They used bench unit data and tracer work to evaluate kinetic parameters and axial dispersion coefficients. Recently, Mosiewski and Morawski (2005) studied hydroconversion of a vacuum residue in a single stirred reactor with dispersed catalyst under continuous operation conditions. They studied the effect of operating parameters such as temperature, hydrogen partial pressure, catalyst concentration and LHSV on residue conversion, asphaltene conversion and hydrodesulfurization. Unfortunately, none of those studies focused in detail on the importance of vaporization in the reactor. Indeed, cracked products can be partially vaporized in the reactor and impact the hydrocarbon liquid residence time, gas hold-up or residue concentration. When conversion increases, cracking is more intense which may result in higher vaporization fractions that have not been quantified yet.

2. Description of the ebullated reactor

Fig. 1 shows the ebullated-bed reactor used in the H-Oil® process to convert and upgrade petroleum residues, heavy oils and bitumen. Temperature typically ranges between 400 and 450 °C while the LHSV of the feed can range from 0.15 to 1.3 h^{-1} depending upon conversion requirements. High temperatures favour cracking of residue molecules and radical formation, while high hydrogen partial pressures favour

* Corresponding author. Tel.: +33 04 78 02 20 97.
E-mail address: thierry.gauthier@ifp.fr (Th. Gauthier).

0009-2509/$ - see front matter © 2007 Elsevier Ltd. All rights reserved.
doi:10.1016/j.ces.2006.12.086

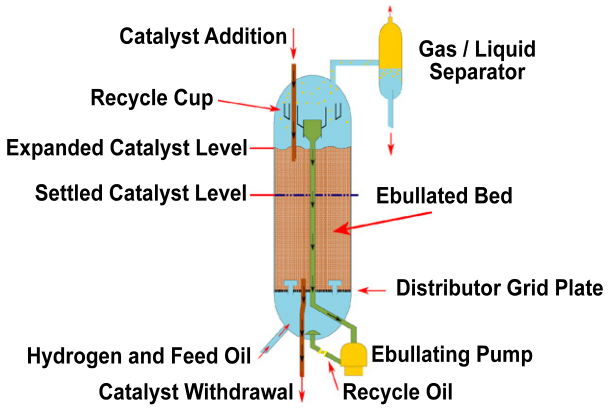

Fig. 1. The ebullated bed-reactor.

hydrogenation of radicals in the presence of a catalyst that promotes hydrogenation to stabilize products and to avoid condensation reactions leading to coke. Concurrently with conversion, purification of products is achieved and high desulfurization and demetallization rates are reported (Colyar, 1997). The hydroconversion process is exothermic. The reactor technology uses a liquid recycle that ensures bed expansion and safely controls the reactor temperature gradient. Individual catalyst particles are therefore maintained in a state of constant motion or fluidized state. This makes it possible to continuously add and withdraw catalyst, and to maintain catalyst activity and stable process performances. The liquid recycle stream is obtained from an internal vapour/liquid separation device (recycle cup) which provides suction to the recycle or ebullating pump (see Fig. 1). The inherent advantages of ebullated-bed reactor are excellent temperature control as well as low and constant pressure drop over several years of continuous operation, since bed plugging and channelling are eliminated through fluidization of the catalyst.

Depending upon performances and design, the H-Oil® process can use several ebullated-bed reactors in series. A gas–liquid inter-stage separator (ISS) can be implemented in between the two reactors to separate gas and liquid products, thus limiting the gas load of downstream reactors (Duddy et al., 2004).

An ISS is implemented between the two ebullated-bed reactors of the hydroconversion bench unit at IFP-Lyon. This allows to evaluate the unit performance in detail by performing mass balances around each reactor separately. Several experimental campaigns were conducted in a wide range of operating conditions with different feedstocks. The purpose of the present study was to carefully estimate vaporization fractions as a function of conversion in order to better describe conversion mechanisms and to evaluate the benefits of Inter-Stage Separation.

3. Experimental

The hydroconversion bench unit located at IFP-Lyon is schematically described in Fig. 2. The reaction zone consists of two elongated reactors (R1 and R2) of 2.2 l operating in ebullated-bed mode loaded with about 700 g of Ni–Mo extrudate catalyst. Temperature is controlled in each reactor by several independent heating zones to maintain a constant reaction temperature along reactors, which is typically in the range of 400–450 °C. At the outlet of each reactor, part of the liquid is degassed and recycled with external pumps to the reactor inlet. The liquid recycle rate is high and represents 25–50 times the fresh feed rate. Hydrogen is introduced upstream of each reactor and mixed with the liquid feedstock to maintain an appropriate hydrogen partial pressure despite hydrogen consumption.

An ISS is implemented between the two reactors to remove the vaporized products from the first reactor. Temperature remains constant from reactor outlet to ISS with careful heat tracing and pressure drop is negligible. Thus, flash conditions in ISS are similar to R1 and allow to evacuate all vaporized hydrocarbons from the liquids. Gas hold-up in R2 is therefore reduced, which favours the residence time of the unconverted hydrocarbons and limits dilution of residue. Downstream the reaction zone, an effluent separation is provided in several stages (flash at high pressure, stripping at atmospheric pressure and vacuum distillation) to collect the different hydrocarbon cuts.

Experiments were conducted at three temperatures from 410 to 440 °C in both reactors. The LHSV of the feed, ranging between 0.15 and 0.3 h^{-1} was adjusted in order to obtain conversions ranging from 30 wt% in R1 to 90 wt% at the outlet of R2. Reactor pressure was maintained at 160 bars in R1 and 156 bars in R2. Hydrogen partial pressure was maintained in the range of 130 bars in each reactor. A vacuum residue representative of Middle East feedstocks was used in the present study. The main properties of the feed are summarized in Table 1. The asphaltene content of the feed reaches 13.2 wt%, whereas metal and hydrogen feed contents are, respectively, around 250 wt ppm and 9.8 wt%.

The bench unit is operated on stream 24 h a day during several weeks and each operating condition was studied during typically 5–7 days. Once the desired operating conditions are reached, mass balances are carried out during periods ranging typically from 10 to 20 h: accurate metering of all gas and liquid streams is carried out; detailed analysis of gaseous streams is performed by using on-line gas chromatography, whereas the liquid composition of each effluent is characterized by simulated distillation in order to determine the net conversion of the residue; sampling of liquid effluents to determine product structures and properties is also performed at two locations, in order to determine the quality of the second reactor feed (R2F) and of the quality of the atmospheric residue (AR) produced by the stripper column. All distillation effluents are carefully collected to conduct further analytical work. Complete mass balances are conducted around R1, R2 and R1+R2. The performances, obtained during a period, are validated only if the global (R1+R2) mass balance accuracy lies between 98 and 102 wt%. The different stream flows are then normalized to account for mass balance discrepancies. Residue conversion is determined based on the quantity of unconverted hydrocarbons boiling above 540 °C. Therefore, conversions in R1, R2 and

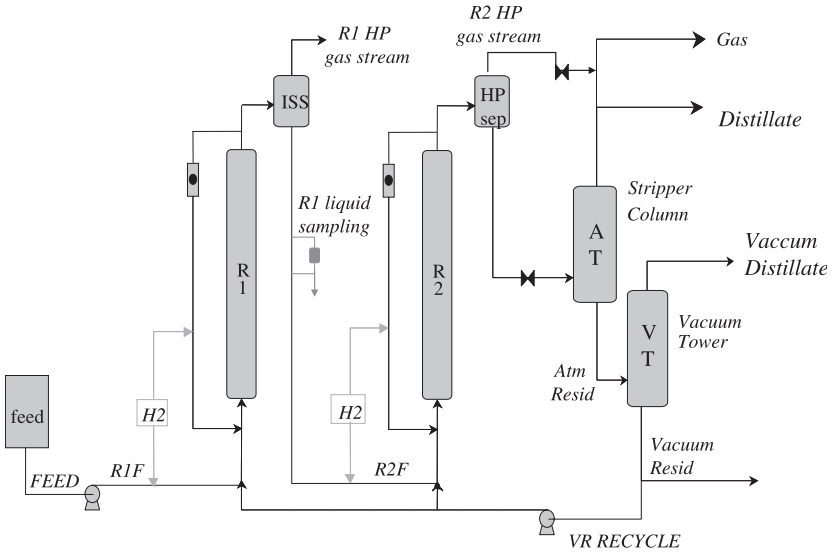

Fig. 2. The ebullated-bed reactor bench unit at IFP-Lyon.

Table 1
Properties of the feedstock used in the study

Feedstock detailed properties		
d 4,15	–	1.045
viscosity (150 °C)	Cst	205
Viscosity (100 °C)	Cst	3500
Nitrogen	wt%	0.387
Sulfur	wt%	5.56
Hydrogen	wt%	9.84
Nickel	wt ppm	59
Vanadium	wt ppl	192
C7 asphaltenes	wt%	13.2
Conradson carbon	wt%	22.9
Distillation		
500 °C	wt%	10
540 °C	wt%	20
560 °C	wt%	26
580 °C	wt%	32

R1+R2 can be defined, respectively, as

$$X_{\mathrm{R1}}^{540\,^\circ\mathrm{C}}(\mathrm{wt\%}) = 100\frac{M_{\mathrm{R1F}}x_{\mathrm{R1F}}^{540\,^\circ\mathrm{C}} - M_{\mathrm{R2F}}x_{\mathrm{R2F}}^{540\,^\circ\mathrm{C}}}{M_{\mathrm{R1F}}x_{\mathrm{R1F}}^{540\,^\circ\mathrm{C}}}, \quad (1)$$

$$X_{\mathrm{R2}}^{540\,^\circ\mathrm{C}}(\mathrm{wt\%}) = 100\frac{M_{\mathrm{R2F}}x_{\mathrm{R2F}}^{540\,^\circ\mathrm{C}} - M_{AR}x_{AR}^{540\,^\circ\mathrm{C}}}{M_{\mathrm{R2F}}x_{\mathrm{R2F}}^{540\,^\circ\mathrm{C}}}, \quad (2)$$

$$X_{\mathrm{R1+R2}}^{540\,^\circ\mathrm{C}}(\mathrm{wt\%}) = 100\frac{M_{\mathrm{R1F}}x_{\mathrm{R1F}}^{540\,^\circ\mathrm{C}} - M_{AR}x_{AR}^{540\,^\circ\mathrm{C}}}{M_{\mathrm{R1F}}x_{\mathrm{R1F}}^{540\,^\circ\mathrm{C}}}. \quad (3)$$

Based on the bench unit mass balance closure and residue concentration analysis, the relative error on conversion can be estimated to be in the range of 2 wt% for experiments conducted on the same feedstock: roughly half of the error comes from the analysis and half from the resid flow estimate which represents typically half of the feed flow rate.

4. Vaporization of hydrocarbons during hydroconversion

The implementation of ISS allows to evaluate the quantity of hydrocarbons vaporized in the first reactor. Indeed, the conditions of the flash in the ISS are very close to R1 conditions. The quantity and composition of the gas phase does not depend upon the internal liquid recycle ratio α (Fig. 3). The gas flow G collected at the ISS therefore corresponds to gas flow at the reactor outlet. The only difference is the liquid flow: the liquid flow at ISS outlet L is different from liquid flow at R1 outlet which is equal to $(\alpha + 1)L$.

The liquid flow at the ISS is given by the bench unit mass balance. The composition of liquid L is determined by high-pressure sampling and subsequent simulated distillation. Vapours G are cooled down and depressurized. Uncondensed fractions are metered and analysed. The flowrate of the condensates is measured and its composition is also analysed by simulated distillation. Fig. 4 gives an example of simulated distillations of liquid bottoms and vapour condensates obtained in conditions where conversion in first reactor $X_{\mathrm{R1}}^{540\,^\circ\mathrm{C}}$ is 67.2 wt%. The flowrates of the different streams are given in Table 2.

There is no information in the literature to support prediction of vapour–liquid equilibria in these extreme conditions. We therefore used the operating data to compute theoretical vapour liquid equilibrium and compared the model predictions to our experimental results. The streams were therefore recombined to carry out flash calculations with various available models.

A breakdown of the hydrocarbon mixture is required to perform flash calculations, in order to represent the heavy hydrocarbon mixture as a combination of several pseudo-components. Apart from H_2, H_2S, CH_4, C_2H_6, C_3H_8 and

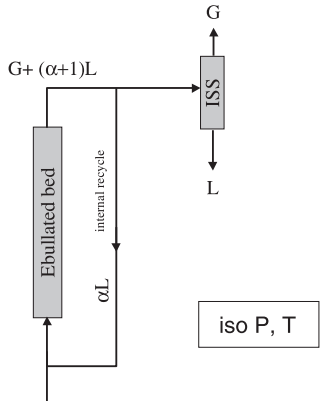

Fig. 3. Gas and liquid flow in R1 and ISS.

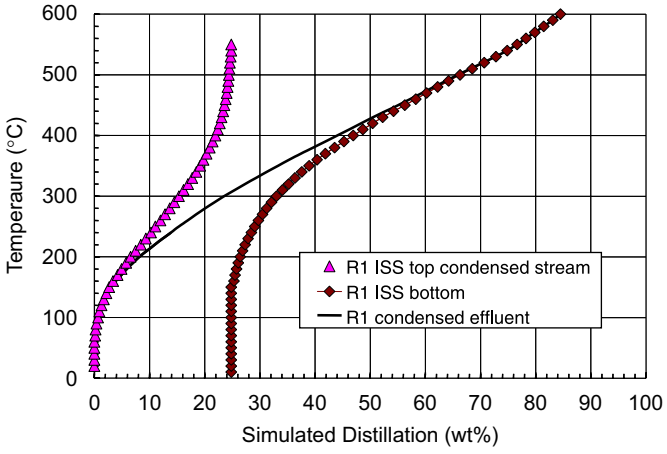

Fig. 4. Composition of liquid fractions at ISS $X_{R1}^{540\,^{\circ}C} = 67.2$ wt%.

Table 2
Flowrates and composition of uncondensed effluent at ISS $X_{R1}^{540^{\circ}C+} = 67.2$ wt%

ISS pressure	(Pa)	$1.60E+07$
ISS temperature	(K)	700.7
ISS bottom liquid	(g/h)	542.2
ISS top condensed liquid	(g/h)	179.1
Uncondensed effluent		
C1 hydrocarbons	(g/h)	8.9
C2 hydrocarbons	(g/h)	7.6
C3 hydrocarbons	(g/h)	12.0
C4 hydrocarbons	(g/h)	7.0
C5 hydrocarbons	(g/h)	4.5
C6+ hydrocarbons	(g/h)	8.3
H_2	(g/h)	28.0
H_2S	(g/h)	30.7

C_4H_{10}, which are individually accounted for, the C_5 and C_6 fractions were characterized by *n*-paraffins, while heavier hydrocarbons were represented as pseudo-components determined by their boiling range. The properties of each pseudo-component were determined based on the mixture boiling range and density assuming a constant Watson characterization factor K, whose definition is shown in Eq. (4). The molecular weight of each pseudo-component was then estimated using the classical Riazi correlation

$$K = \frac{\sqrt[3]{1.8(T_{50} + 273.15)}}{spgr}. \quad (4)$$

The flash calculations were conducted using two thermodynamic models: Grayson–Streed (GS) and Peng–Robinson (PR) standard model provided in PRO II 5.5 simulation software. The boiling range of each pseudo-component was fixed to 50 °C in order to avoid any significant numerical impact on the results. The main error associated to the vapour–liquid equilibrium calculation is probably due to the pseudo-component estimates using the common and constant characterization factor K for each component equal to the K factor of the feedstock which could not be checked in this particular case. Table 3 shows the results of the breakdown and the results of flash calculations in the conditions defined above. They were compared with experimental data provided by the ISS mass balance.

As shown in Table 3, the experimental concentrations of dissolved gases could not be determined due to losses during depressurization of the high-pressure samples, although they are accounted for in the liquid flowrate. It can be shown that the impact on the dissolved fraction is negligible (less than 1 wt% of the hydrocarbons lighter than C6 are dissolved in liquids, as shown in Table 3). Therefore, both thermodynamic models predict rather well the composition of the gas stream leaving the ISS. However, the GS model significantly underestimates the vaporization fraction, while the PR model works very well.

The same flash calculations were conducted over a wide range of conversions in R1 ranging from 35 to 70 wt%, based on experimental compositions at the ISS inlet. When conversion increases, there are more light hydrocarbons and less heavy fractions in the R1 effluents. Hence, the vaporization fraction at the ISS increases from 15 to 40 wt%. Fig. 5 shows a comparison between experimental vaporization fractions and vaporization fractions predicted with both models. The GS model systematically underestimates vaporization by 10%, but the PR model matches the experimental findings very well over the range of conditions tested.

Based on the composition of the effluents, we can therefore determine the vaporization fraction at the outlet of R1 even in the severe operating conditions of the present study. We applied the same methodology to calculate the vaporization fraction of the R2 effluents, which cannot be measured experimentally since downstream separation is carried out at lower temperature. We also computed the vaporization fraction that would be obtained at R2 outlet without ISS by integrating R1 vapours into the feed to R2. The vaporization fractions are represented as a function of $X_{R1}^{540\,^{\circ}C}$ for R1, and $X_{R1+R2}^{540\,^{\circ}C}$ for R2 in Fig. 6.

Fig. 6 clearly shows the impact of the ISS on the vaporization fraction. In R2, the overall conversion level can be quite high, above 70 wt%. Hence, without inter-stage separation, very high vaporization fractions above 40% would be observed at the R2 reactor outlet. With inter-stage separation, the vaporization fraction drops, since light hydrocarbons produced in R1 bypass second reactor.

Table 3
Flash calculation at ISS: $X_{R1}^{540\,^{\circ}C} = 67.2$ wt%

	R1 effluent		Liquid phase			Vapour phase		
	MW (g/mol)	x (wt%)	GS x (wt%)	PR x (wt%)	Exp x (wt%)	GS x (wt%)	PR x (wt%)	Exp x (wt%)
C1	16.04	1.07	0.09	0.08	0.00	3.49	3.00	3.11
C2	30.07	0.92	0.15	0.09	0.00	2.84	2.53	2.67
C3	44.10	1.44	0.23	0.18	0.00	4.44	3.90	4.18
C4	58.12	0.85	0.16	0.12	0.00	2.56	2.26	2.45
C5	72.15	0.54	0.12	0.10	0.00	1.59	1.41	1.58
C6	86.18	1.00	0.27	0.21	0.00	2.82	2.55	2.91
H_2	2.02	3.38	0.26	0.18	0.00	11.09	9.57	9.77
H_2S	34.08	3.71	0.40	0.42	0.00	11.88	10.08	10.73
123–150	118.40	2.53	0.98	0.83	0.00	6.38	5.83	6.78
150–200	140.80	4.70	2.21	1.94	2.14	10.87	10.06	9.79
200–250	173.00	6.23	3.69	3.42	3.51	12.52	11.70	11.32
250–300	210.80	7.17	5.46	5.13	5.26	11.39	11.12	10.76
300–350	254.10	8.41	8.14	7.60	7.85	9.08	9.98	9.69
350–400	304.60	9.38	10.91	10.26	10.64	5.58	7.66	6.99
400–450	363.90	9.60	12.48	12.10	12.46	2.47	4.73	4.15
450–500	432.60	9.44	12.93	13.05	13.31	0.81	2.44	2.03
500–550	511.30	9.21	12.86	13.39	13.76	0.19	1.10	1.08
550–995	909.60	20.41	28.66	30.90	31.07	0.00	0.07	0.00
Vaporization ratio (wt%)						28.79	34.01	34.54

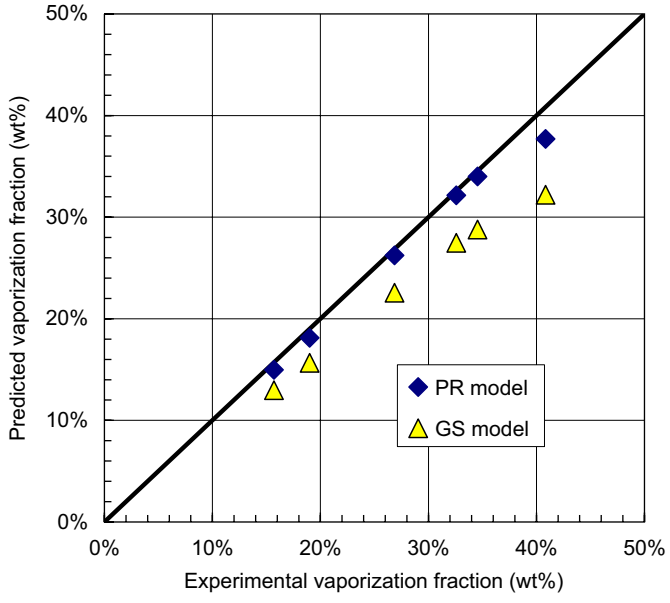

Fig. 5. Experimental and predicted vaporization rates at different conversion levels.

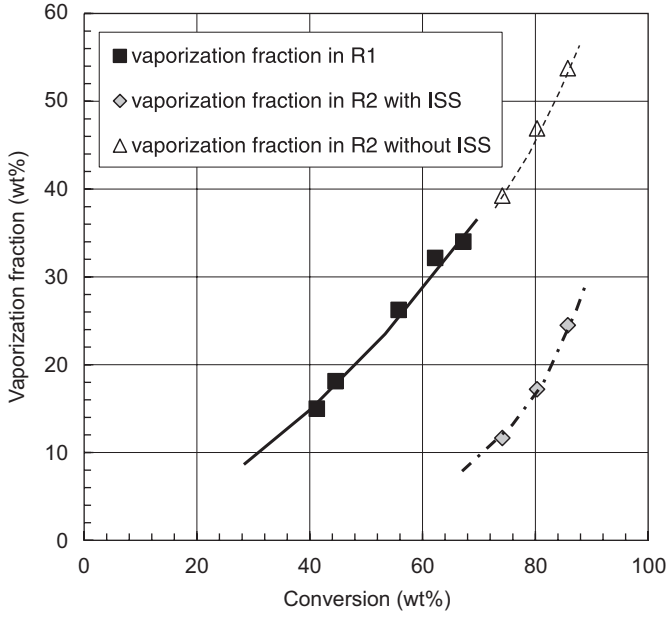

Fig. 6. Vaporization fractions as function of conversion.

Accounting for the liquid recycle allows to calculate the vaporization fraction β_R that occurs in the reactor from the vaporization fraction β at the reactor outlet by taking the internal recycle into account:

$$\beta_R = \frac{\beta}{\alpha + 1}. \tag{5}$$

On the bench unit, the liquid recycle ratio α is typically 40. In industrial units, however, the liquid recycle ratio α can be 10 times lower due to differences in design. Therefore, in the bench unit, at the same vaporization fraction, the gas hold-up inside the reactor will remain low, in the range of 1–2 wt% of the flow. In industrial ebullated-bed reactors, however, gas hold-up may reach values higher than 10 wt% in the same conditions. Hence, vaporization has to be explicitly accounted for to describe the hydroconversion process and to scale-up data from bench units to industrial units. Indeed, vaporization will strongly impact reactor hydrodynamics, as vaporized hydrocarbons

exit the reactor more rapidly than liquids because they flow in bubbles. Furthermore, the amount of gas in the reactor also affects the space available for liquids in the reactor and hence the reactor hydrodynamics. If the gas void fraction is too high, coalescence leading to turbulent bubbling or even foaming can be observed (McKnight et al. (2003)).

5. Modelling of hydroconversion

Mosiewski and Morawski (2005) have found that conversion mainly depends upon space velocity of the feed and temperature, and that hydrogen partial pressure and catalyst concentration do not influence conversion significantly. This clearly illustrates that hydroconversion is initiated by thermal cracking of residue while catalytic hydrogenation stabilizes radicals that are formed. Conversion reactions mainly occur in the liquid phase since vapours leave the reactor almost immediately as bubbles. In order to model the conversion process, it is therefore necessary to correctly describe the liquid phase hydrodynamics and to determine the actual residence time of liquid hydrocarbon fractions in the reactors. Since vaporization of hydrocarbons is very significant, it may modify hydrodynamic characteristics such as gas hold-up or liquid flowrate. Therefore, vaporization may have to be accounted for in order to describe liquid residence time and residue concentration in the reactor.

Ebullated-bed reactor hydrodynamics can be described by an axial dispersion model (Schweitzer and Kressmann, 2004). When considering the ebullated-bed reactor together with its internal recycle, however, the overall liquid hydrodynamics can be represented by a simple CSTR. Indeed, Fig. 7 shows the cumulative residence time distribution function $F(t)$ of a plug flow reactor with a recycle ratio α equal to 40, corresponding to a typical bench unit operation. The function $F(t)$ with recycle is very similar to that of an equivalent CSTR. This approach

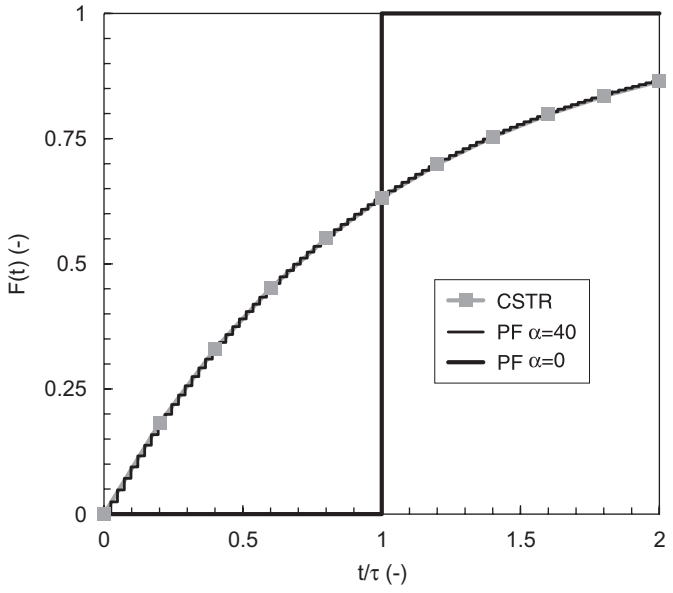

Fig. 7. Cumulative residence time distribution function of ebullated-bed reactor compared to plug flow and CSTR reactors.

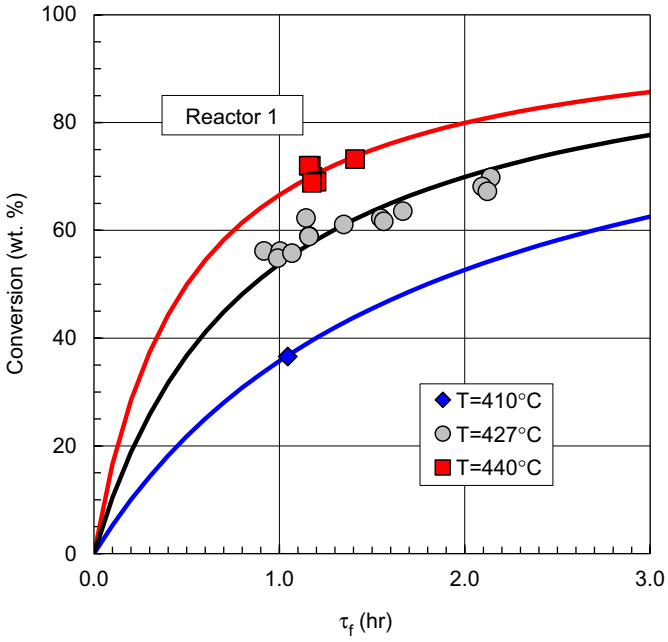

Fig. 8. Residue conversion $X_{R1}^{540\,^{\circ}C}$ in R1 as a function of feed residence time. Lines represent fitted first order conversion kinetics for R1.

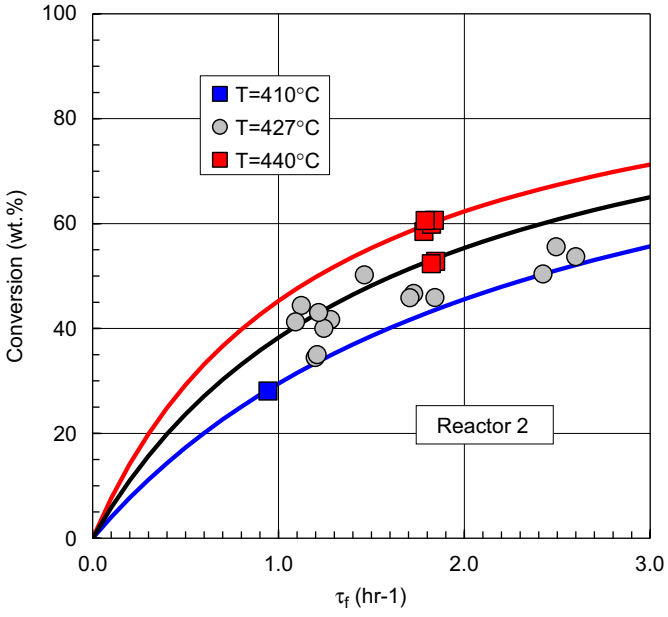

Fig. 9. Residue conversion $X_{R2}^{540\,^{\circ}C}$ in R2 as a function of feed residence time. Lines represent fitted first order conversion kinetics for R2.

is valid for isothermal operation as long as the recycle ratio remains high enough. As a consequence, liquid flow in each reactor stage, comprising the ebullated-bed reactor and the recycle line, can be represented by a CSTR flow.

The tests on the bench unit were conducted over a wide range of temperatures and space velocities in order to vary residue conversion from 35 to 90 wt%. In Figs. 8 and 9 residue conversion in each reactor of the bench unit is represented as a

function of the residence time of the feed τ_f in R1 and R2. The residence time of the feed is defined here without accounting for vaporization as a function of available space in the reactor (Eq. (6)), while the feed flowrate is expressed in standard conditions. These are convenient assumptions, which do not account for the actual liquid flow structure, however. In the bench unit, due to high recycle ratios, the gas volumetric fraction ε_g is small and accounts for less than 5% of the reactor volume. The loaded catalyst volumetric fraction ε_s accounts for 17% of the reactor volume

$$\tau_f = \frac{V_r(1-\varepsilon_g-\varepsilon_s)}{Q_f^{15\,^\circ\mathrm{C}}}. \tag{6}$$

Both temperature and hydrocarbon residence time impact on conversion as shown in Figs. 8 and 9. Three different temperatures were studied, increasing from 410 to 440 °C. One can see that temperature impact is larger in R1 than in R2: with a residence time τ_f equal to 2 h, an increase of temperature from 410 to 440 °C will increase conversion by 30 wt% in R1 and by 20 wt% only in R2. Furthermore, at similar operating conditions, conversions are smaller in R2 than in R1. If we consider a single first order conversion kinetics to describe hydroconversion without significant vaporization, we should observe similar performances in both reactors. This is not the case and suggests that a more detailed description of reaction conditions is needed to account for residence time variations of the liquid related to vaporization, but also to describe the difference in feedstocks between R1 and R2 through the residue concentration.

In order to correctly model conversion, we have to improve the description of the operating conditions in the reactor accounting for vaporization. As it is difficult to make a molecular description of residue concentration, a pseudo-kinetic expression for conversion was therefore considered to follow the evolution of residue concentration expressed in mass fraction as a function of conversion. Hydrogen partial pressure did not vary significantly during the experiments. This parameter was therefore not considered

$$r_{540\,^\circ\mathrm{C}} = k_0 \mathrm{e}^{-Ea/RT}\left[C^{540\,^\circ\mathrm{C}}\right]^n. \tag{7}$$

Eq. (7) was combined with the continuity equation of the reactor to calculate conversion as a function of true liquid residence time, assuming that liquid is completely mixed (CSTR), as discussed before, and that the residence time in the vapour phase is negligible. The true liquid residence time of hydrocarbons was expressed to account for true liquid volumetric flow and vaporization:

$$t_c = \frac{V_r(1-\varepsilon_g-\varepsilon_s)}{Q_f^T(1-\beta)}. \tag{8}$$

The conversion data obtained in the first reactor were used to determine the kinetic constants k_0 and E_a, for a given order of reaction n. The kinetic constants determined from the R1 data were then used to simulate R2 operation. Figs. 10 and 11 show

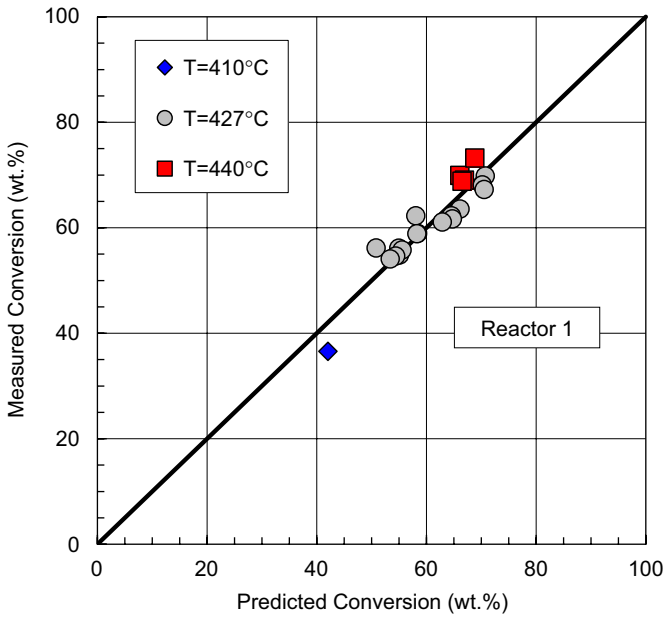

Fig. 10. Predicted vs. measured conversion in R1 (order of reaction $n = 1$).

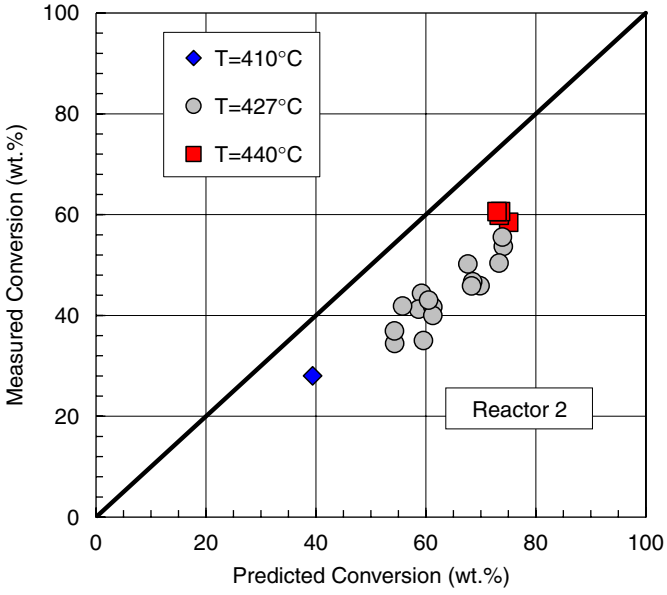

Fig. 11. Predicted vs. measured conversion in R2 (order of reaction $n = 1$).

the results obtained with an order n equal to 1. The R1 data are correctly described by adjusting the kinetic parameters (Fig. 10). However, it is not possible to predict R2 conversion as it is overestimated when using the R1 kinetic parameters (Fig. 11). Hence, it was decided to modify the reaction order to account for the large variation in reactivity of the various feed components. Several reaction orders were attempted to match both R1 and R2 performance and it was found that conversion can best be described by a reaction order n equal to 2, as shown in Figs. 12 and 13. As shown by Ho and Aris (1987), apparent second order reactions can arise when a reacting lump is composed of several species of different reactivity. As the more

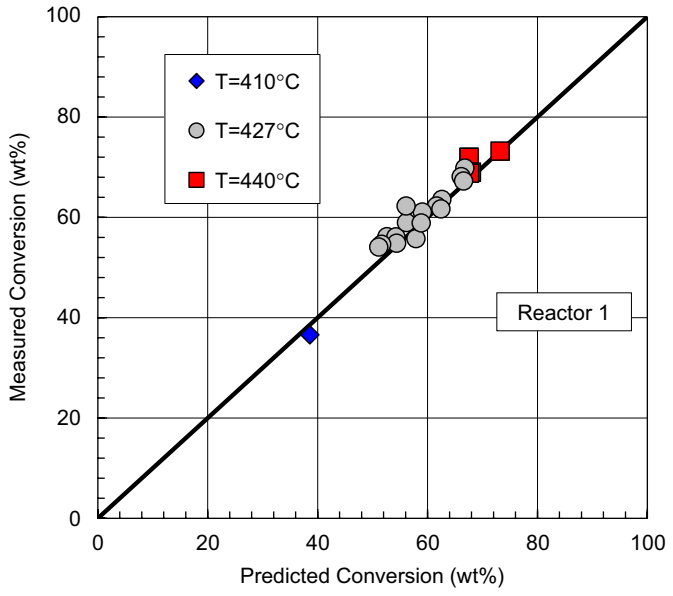

Fig. 12. Predicted vs. measured conversion in R1 (order of reaction $n = 2$).

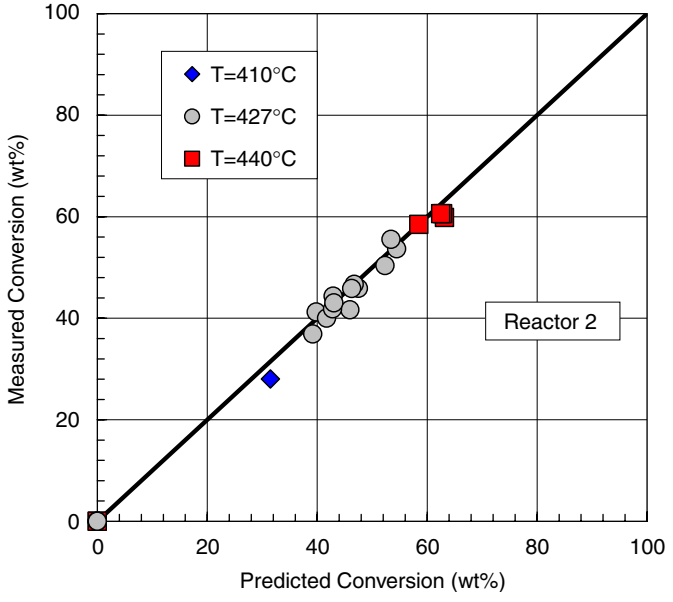

Fig. 13. Predicted vs. measured conversion in R2 (order of reaction $n = 2$).

reactive species are depleted, the first order rate constant will decrease with increasing conversion (Nagaishi et al., 1997). Several parallel first order reactions probably occur during hydroconversion. Our results therefore show that the conversion can be simply represented by a second order kinetics allowing to describe the complete conversion range with the same rate constant.

6. Conclusion

Vaporization of hydrocarbons during hydroconversion at severe conditions can be very significant depending upon conversion level. Despite extreme operating temperature and pressure, it is possible to correctly estimate the vaporization fraction with the PR model.

Vaporization results in higher gas hold-up at large scale due to differences in unit design and operation. This phenomenon is essential and needs to be taken into account during scale up considerations.

Vapour flow in two-stage ebullated-bed units can be controlled by inter-stage vapour removal. This reduces second stage gas-load and favours hydroconversion conditions.

An enhanced description of reaction conditions by including vaporization also enables to better describe hydroconversion kinetics. Our data suggest that hydroconversion can be adequately represented by a second order kinetics.

Notation

C	concentration, kg/kg
E_a	activation energy, J/mol/K
G	vapour mass flow rate, kg/s
k_0	hydroconversion kinetic constant, s^{-1}
K	Watson characterization factor, dimensionless
L	liquid mass flow rate, kg/s
M	mass, kg
Q	volumetric flow rate, m^3/s
r	reaction rate, $kg/m^3/s$
t	time, s
T	reaction temperature, K
V	volume, m^3
x	weight fraction, dimensionless
X	conversion, wt%

Greek letters

ε	volumetric fraction, dimensionless
τ	residence time, s

Acknowledgements

The authors would like to acknowledge Cyril Collado, Alain Ranc, Lisebelle Jussaumes and Jean-Charles De Hemptinne for their contribution, help and advice to this work.

References

Colyar, J.J., 1997. Ebullated Bed Reactor Technology. Upgrading heavy Ends with IFP. Institut Français du Pétrole, Rueil Malmaison, pp. 41–49.

Colyar, J.J., Wisdom, L.I., 1997. The H-Oil process, a worldwide leader in vacuum residue processing. In: Proceedings of the National Petroleum Refiners Association Annual Meeting, San Antonio, TX.

Duddy, J.E., Wisdom, L.I., Kressmann, S., Gauthier, T., 2004. Understanding and optimization of residue conversion in H-Oil®. In: Proceedings of the Third Bottom of the Barrel Technology Conference (BBTC), October 20–21, Antwerp, Belgium.

Flint, L., 2004. Oil Sands Technology Roadmap, Unlocking the Potential. Alberta Chamber of Resources.

Ho, T.C., Aris, R., 1987. On apparent second-order kinetics. A.I.Ch.E. Journal 33 (6), 1050–1051.

McKnight, C., Hackman, L., Grace, J.R., Macchi, A., Kiel, D., Tyler, J., 2003. Fluid dynamic studies in support of industrial three phases fluidized bed hydroprocessing. Canadian Journal of Chemical Engineering 81, 338–350.

Mosiewski, J.M., Morawski, I., 2005. Study on single-stage hydrocracking of vacuum residue in the suspension of Ni–Mo catalyst. Applied Catalysis A: General 283, 147–155.

Nagaishi, H., Chan, E.W., Sanford, E.C., Gray, M., 1997. Kinetics of high conversion hydrocracking of bitumen. Energy & Fuels 11, 402–410.

Schweitzer, J.M., Kressmann, S., 2004. Ebullated bed reactor modeling for residue conversion. Chemical Engineering Science 59, 5637–5645.